Springer

Journal of Mechanical Science and Technology 23 (2009) 2529~2547

Journal of Mechanical Science and Technology

www.springerlink.com/content/1738-494x
DOI 10.1007/s12206-009-0711-y

A review of the critical heat flux condition in mini-and microchannels †

Anand P. Roday and Michael K. Jensen*

Department of Mechanical, Aerospace and Nuclear Engineering, Rensselaer Polytechnic Institute ,Troy, NY, 12180, USA

(Manuscript Received May 8, 2008; Revised May 11, 2009; Accepted May 11, 2009)

Abstract

With ever increasing power dissipation in electronic chips that are shrinking in size, cooling demands are becoming more severe. Forced air cooling is reaching its operational limits, and single-phase liquid cooling in microchannels has been able to accommodate the rising heat fluxes. Further increases in computing (chip) power suggest that a switch from single-phase to boiling heat transfer will be needed. A major impediment to using boiling or forced convective vaporization for such a cooling application is the limiting critical heat flux (CHF) condition. In this paper, the CHF condition in microchannels is reviewed. Data from the literature are discussed, and new data for a range of operating and geometric conditions are presented. Influencing factors, parametric trends, phenomenological models, and other aspects of the CHF condition are discussed.

Keywords: Boiling; Critical heat flux; Dryout; Heat transfer coefficient

1. Introduction

Progress in the past few years toward better cooling approaches for electronic equipment has been driven indirectly by the consequences of Moore's Law [1], which states that the number of transistors in an integrated circuit (IC) doubles every 18 months. This progress has resulted in dramatic increases in packaging density and performance, but this significantly greater IC chip power has resulted in heat fluxes from about 50 W/cm^2 in current electronic chips to about 2000 W/cm^2 [2] in semiconductor lasers. The groundbreaking work of Tuckerman and Pease [3] in 1981 using the flow of water in 50-μm wide and 300-μm deep microchannels demonstrated the possibility of accommodating such high heat fluxes through the use of very small channels. Likewise, with developments in nanotechnology, fuel cell technology, the desire for reduced weight in the aerospace industry, etc., heat exchangers dramatically more compact than traditional compact heat exchangers are being designed with surface area densities as high as 10,000 m^2/m^3 [4]. Such high surface densities can be achieved using a large number of small channels in the 100-1,000-μm range, channels in the so-called mini- and microchannel range [5].

The challenge of cooling electronic devices is that chip temperatures must be maintained below 85°C despite the high local heat fluxes. This imposes a practical limit on traditional cooling approaches such as natural and forced convection using air. Adoption of liquid cooling (with or without phase change) seems to be a viable option, and the use of boiling has many attractive features from a thermal perspective, such as reduced flow rates (taking advantage of enthalpy of vaporization), lower temperature differences, and improved temperature uniformity. Designers of non-electronic heat transfer applications also have recognized the value of the same positive heat transfer attributes of flow boiling in small channels.

Thus, boiling heat transfer in small channels is a potential solution to some thermal control (cooling) and thermal processing applications (compact heat exchangers). However, flow boiling in tubes and

† This paper was recommended for publication in revised form by Associate Editor Jae Young Lee

*Corresponding author. Tel.: +1 518 276 2843, Fax.: +1 518 276 6025
E-mail address: JenseM@rpi.edu

channels is a quite complex process with some limitations on its use. In particular, an upper operational limit on the heat flux is defined as the critical heat flux (CHF) condition, at which a wet-wall, high heat transfer coefficient operating condition transitions to a dry-wall, low heat transfer coefficient situation.

For conventional size channels, the CHF condition has been extensively investigated. Despite the vast number of studies carried out, the CHF condition is still not completely understood. Considerable differences are found to exist in the practical methods used to define and measure the CHF condition. Because of the complexity of the mechanism, few satisfactory analytical treatments are available, and the majority of the literature on this subject relies on experimental data for different geometries and fluid conditions. Bergles [6] has estimated that several hundred thousand data points have been obtained in such studies and over 200 correlations have been developed (e.g., Macbeth [7], Bowring [8], the Heat and Mass Transfer Section of the Scientific Council, USSR Academy of Sciences [9], Katto and Ohno [10], Groeneveld et al. [11], Hall and Mudawar [12]). Applicability of these correlations to smaller diameter tubes (< ~1 mm) is problematical; likewise, most of the correlations were developed for flow boiling of water.

As is the case for larger diameter tubes, the limiting operational factor for flow boiling in mini- or microchannels is the CHF condition. However, the CHF literature for small passages is quite limited with contradictory results. This literature, discussed below, focuses on small hydraulic diameter channels (about 2 mm and below). In addition, new data from our lab for tubes from 0.28 to 0.70 mm are presented and discussed.

2. Overview of boiling and CHF studies in microchannels

CHF studies can be grouped into studies in single and parallel microchannels. Jiang et al. [13] investigated phase-change in microchannel heat sink systems consisting of either 34 or 35 microchannels made of silicon. The micro-channels were V-grooved with hydraulic diameters of 40-μm or 80-μm. They concluded that due to the microscale size of the channels, a stable vapor core was established in the microchannel at an early stage such that the evaporation at the liquid film-vapor core interface became the dominant heat transfer mechanism. The typical bubbly flow where the bubbles form, grow and detach from the channel wall was suppressed. Usually, the bubble activity keeps the wall temperature relatively uniform with increasing heat flux resulting in a "plateau" in the boiling curve (T vs. q''), but Jiang et al. did not observe such a boiling plateau, as is the case in large-sized channels; here, the slope of wall temperature versus heat flux plot gradually decreased until the CHF condition was reached, and then the temperature increased sharply as is seen in Fig. 1. As with the study by Yen et al. [14] in single circular tubes discussed later, the exit quality at CHF was found to be about 1.0, with the channel flow in single-vapor phase. However, the authors have not reported the critical heat flux values obtained from their experiments.

Bowers and Mudawar [15] conducted studies with R-113 in circular mini-channel and micro-channel heat sinks made of copper. The micro-channel heat sink had 510 μm diameter channels; however, the number of parallel micro-channels was not stated. The heat sink housing, to which the heater was soldered, had both inlet and outlet plenums that were large enough to ensure uniform pressures in the plena.

Assuming equal flow rates through the individual channels, they concluded that the CHF was not a function of inlet subcooling. CHF increased with mass velocity. At very low flow rates the experiment produced superheated vapor exit temperatures even at heat fluxes lower than the CHF. The authors believed that heat was conducted away from the downstream region undergoing CHF to the boiling region of the channel, and that it is thus possible to achieve an evaporation efficiency of unity (low coolant flow rate) in flow boiling with miniature heat sinks.

Qu and Mudawar [16] measured the CHF for a water-cooled microchannel heat sink that contained 21

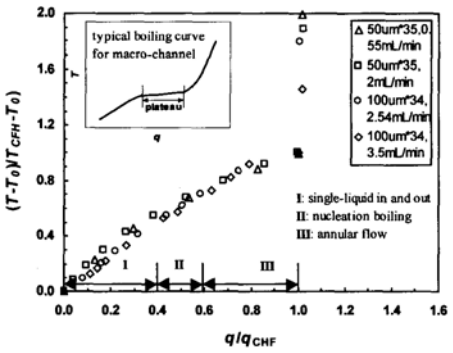

Fig. 1. Boiling curve for microchannel heat sink [13].

parallel 215×821 μm channels over a mass velocity range of 86-368 kg/m^{2}s, inlet temperatures of 30 and 60°C, and outlet pressure of 1.13 bar. The CHF condition increased with an increase in mass velocity and was independent of inlet temperature. Based on these data, and from previous experiments with R-113 [15], they proposed a new correlation for CHF.

Flow instabilities can severely affect the tests conducted to determine the CHF condition, and instabilities need to be addressed when performing the CHF experiments. There are three major instabilities that affect microchannel heat exchangers—the upstream compressible volume instability, the excursive instability, and the parallel channel instability. The upstream compressible volume instability occurs when there is a significant compressible volume upstream of the heated section which causes severe pressure drop oscillation leading to a premature CHF. This compressibility could be due to an entrained gas bubble, a flexible hose, or the presence of a large volume of degassed liquid upstream of the small microchannel [17]. Throttling the inlet helps to eliminate this instability by isolating the microchannel from the compressible volume. With the absence of an upstream throttle valve, as was the case in studies by Jiang et al. [13] and studies by Bowers and Mudawar [15], the compressible volume instability could be likely responsible for a reduced CHF value.

Qu and Mudawar [16] took care to address this instability by installing a throttle valve upstream of the heat-sink and found that severe flow oscillations occurred when the valve was open; by throttling this valve, the oscillations were virtually eliminated. However, Qu and Mudawar observed an unusual phenomenon as CHF approached; there was vapor backflow from all the channels towards the inlet plenum as is seen in Fig. 2, and this was responsible for the lack of inlet subcooling effect seen in the CHF data as mentioned previously.

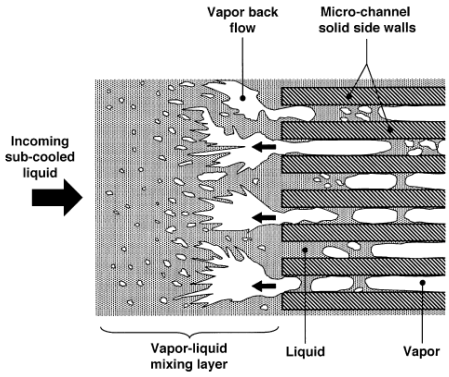

Fig. 2. Vapor back flow in the experiments of Qu and Mudawar [16].

As pointed out in [17], it is quite likely that Qu and Mudawar's upstream throttling took care of the compressible volume instability, but their experiment was still subject to parallel channel instability which is closely connected with the second kind of instability called the excursive instability. This instability occurs if the pump (supply) characteristics (pressure drop vs. mass flow rate curve), as seen by the heated microchannel, has less of a negative slope than the test-section curve, which ultimately leads to the system being unstable, shifting the equilibrium point to such a low flow rate that the critical heat flux condition occurs. This can be avoided by increasing the available pressure drop (supply) in conjunction with a throttle valve so that a stable operation is possible. In case of single microchannels, this can be taken care of by having a very high upstream pressure drop as is seen in the studies described in a subsequent section by Roday et al. [18] and shown in Fig. 7.

In the case of parallel microchannels, improved fabrication techniques can be used to employ flow restrictions at the inlet of each channel to accomplish the pressure drop needed and, thus, avoid excursive instabilities observed by Qu and Mudawar [16]. This technique was used by Koşar et al. [19], who employed inlet restrictors to study the suppression of flow boiling oscillations in a silicon microchannel device having five channels of size 200-μm wide and 264-μm deep, 1 cm long. Five 20-μm wide MEMS-based microfabricated orifices were installed at the entrance of each channel and their lengths were varied from 0 to 400-μm to study the effect on suppressing flow instabilities.

They observed severe pressure drop oscillations in the unrestricted device (1NR) at the onset of unstable boiling (OUB). With a progressively larger inlet restriction (2R50, 3R200, 4R400), the severity of the pressure drop oscillations decreased, such that no significant pressure drop oscillations (<1 kPa) were obtained for the device 4R400.

Higher heat flux values were obtained at OUB for the devices with restrictors when compared to the unrestricted device for the same mass flux indicating that the parallel channel and upstream compressible volume instabilities can induce premature CHF. The OUB for the restriction 4R400 was directly associated

with the CHF condition.

Using a pressure drop multiplier parameter, M

$$M = (\Delta p_{microchannel} + \Delta p_{orifice}) / \Delta p_{microchannel} \quad (1)$$

Koşar et al. [19] demonstrated that the value of CHF increased with an increase in restrictor length, as shown in Fig. 3.

Using the same device as in [19], Koşar and Peles [20] studied the CHF condition of R-123 at exit pressures ranging from 227 kPa to 520 kPa. CHF data were obtained over heat fluxes from 53 to 196 W/cm^2 and mass fluxes from 291 to 1118 kg/m^{2}s. Flow images and high exit qualities suggested that dryout was the leading CHF mechanism. CHF increased fairly linearly with mass flux. A detailed discussion on the parameters affecting the CHF in this study is discussed in a later section on parametric effects on CHF.

Kuan and Kandlikar [21] studied the effect of flow boiling stability on CHF with R-123 in six parallel microchannels of hydraulic diameter 546.5-μm (cross sectional area of each microchannel is 1054-μm ×157-μm) machined on a copper block of dimensions 88.9 mm × 29.6 mm. They studied the effect of using pressure drop elements (PDE) by using a manifold which had inlet openings of 127-μm diameter at the inlet to each channel, giving an open area that was 7.7% of the cross sectional area of the 1054-μm ×157-μm channel. These flow restrictors were expected to help reduce vapor backflow; however, no visual flow patterns were reported. Their results show a decrease in the CHF value with the use of restrictors as shown in Fig. 4, which is contrary to what is expected and to the results by Koşar et al. [19, 20]. Since the actual design of the restrictors is not well described, the reasons for this behavior are not clear.

Conjugate heat transfer effects can become important in microchannels since the channel wall thickness becomes comparable to the microchannel size. For microchannels fabricated on large blocks, it is possible that there is significant axial and longitudinal conduction through the substrate. This results in a redistribution of heat flux away from those locations where the CHF condition typically initiates (i.e., at the exit) and eventually leads to the CHF condition occuring at the hottest surface. Higher values of the apparent CHF could be obtained due to these conjugate effects. Numerical studies of conjugate heat transfer with single-phase flow in microchannels have

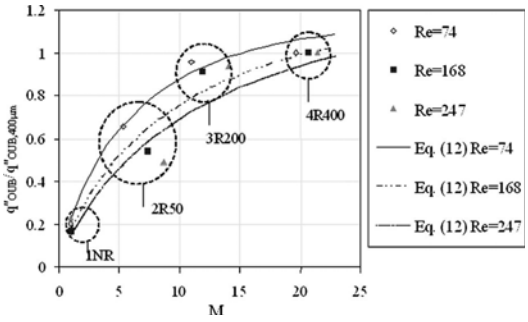

Fig. 3. $q''_{OUB}/q''_{OUB,\ 400\ \mu m}$ as a function of M [19].

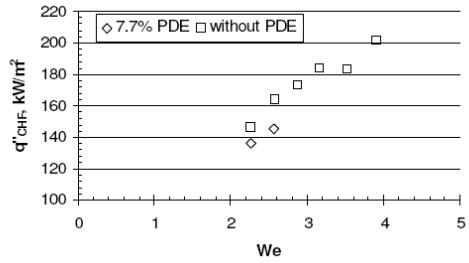

Fig. 4. Critical heat flux vs. Weber Number with and without pressure drop elements (PDE) (Kuan and Kandlikar [21].

been conducted (e.g., Rostami [22]), but such studies for two-phase flow and the effects on CHF have not been reported. It is difficult to place temperature sensors around the circumference of a MEMS-based microchannel device to obtain local wall temperature and heat flux as pointed out by Bergles and Kandlikar [17]; hence, numerical techniques might have to be used to study conjugate effects in parallel microchannels. In single circular tubes, conjugate effects on CHF could be experimentally studied by selecting test sections with the same inside diameter but varying the wall thickness and material.

There are very few CHF investigations in small circular tubes. There have been some studies in tubes with small dimensions (down to about 0.3 mm) involving very high mass velocities intended for extremely high heat flux removal as in fusion reactors [23-26], but studies at lower mass fluxes, typical of electronics cooling application, are very limited. For example, Celata et al. [25] have conducted subcooled CHF studies in tube diameters as small as 0.25 mm for very high heat fluxes (up to 70 MW/m^2) and high mass fluxes (greater than 5000 kg/m^{2}s) for fusion technology application. Nariai et al. [26] reported CHF studies with water at ambient exit pressure in stainless steel tubes with inside diameter of 1 mm, 2

mm and 3 mm; tests were performed from the subcooled to the quality region (very close to zero quality) for mass fluxes ranging from 7,000 to 11,000 kg/m^2 s. They indicated that the CHF decreased with an increase in exit quality in the subcooled region (i.e., negative quality indicated subcooled liquid). There was a minimum in the CHF versus quality curve very close to zero quality. As quality was further increased to a positive value the CHF increased sharply.

A similar trend was observed by Bergles et al. [27] for CHF with de-ionized water in a stainless steel 2.38 mm tube with L/d=15, mass flux of 3000 kg/m^2 s, and an exit pressure of 207 kPa. At high subcooling CHF decreased monotonically with increases in quality; the data passed through a minimum and then increased in the bulk boiling region. Bergles et al. argued that at low values of subcooling the void fraction became appreciable, which caused an increase in average velocity with the result that the burnout limit was raised. They also investigated the effect of diameter on CHF for tube diameters from 0.58-mm to 4.58-mm and found a strong inverse dependence of CHF on diameter. The earlier work by other researchers suggested that CHF decreased with decrease in diameter, when the size was reduced below 2-mm. Bergles et al. argued that this could be due to flow oscillations caused by the upstream compressibility of the loop.

Roach et al. [28] studied the CHF associated with flow boiling of subcooled water in circular tubes with diameters of 1.17 mm (L/d=137) and 1.45 mm (L/D=110), mass velocities from 250 to 1000 kg/m^{2}s, exit pressures from 345 to 1035 kPa, and inlet temperatures from 49 to 72^{o}C. They observed the CHF condition to occur at very high exit qualities (around 0.8) indicating dry-out. CHF increased with increasing channel diameter, mass flux and pressure. They found that in both the tube sizes for pressure around 690 kPa and mass flux about 800 kg/m^{2}s, CHF did not occur at all, and a smooth transition from nucleate to film boiling took place. They stated that the channel exit pressure and mass flux could not be maintained constant during the tests, which indicates an unstable flow and, thus, the CHF results could be based on an unstable flow condition.

Oh and Englert [29] conducted sub-atmospheric CHF experiments with water in a single rectangular aluminum channel heated on one side with electric strip heaters. Their channel cross-section dimensions were 1.98 mm × 50.8 mm (hydraulic diameter of 3.8 mm) and heated length of 600 mm (L/D=160). The exit pressures ranged from 20 kPa to 85 kPa. The tests were performed with mass fluxes from 30 to 80 kg/m^{2}s. CHF was found to increase with mass flux in almost a linear fashion. The relation between subcooling and CHF was also found to be linear although the effect was not significant. For an inlet subcooling up to 66 K, CHF increase was just 15 %.

CHF experiments were performed by Lazarek and Black [30] with R-113 in a stainless steel tube of inside diameter 3.15 mm (L/d=40) in a vertical orientation. The tube had a heated length of 12.6 cm and a wall thickness of 0.40 mm. The pressure varied from 124 kPa to 414 kPa. The mass velocities were in the range of 140 to 740 kg/m^{2}s. Inlet subcooling varied between 3 to 73^{o}C. They found that the CHF occurred at very high exit qualities (from 0.5 to 0.8). Following the power increase, the wall temperatures underwent progressively large oscillations due to intermittent rewetting of the passage wall. CHF occurred because of the dryout of the liquid and always at the exit of the heated test section length. Axial conduction effects on CHF were not assessed in this study even though the test section had a thick wall.

Yu et al. [31] carried out CHF experiments with water in a stainless steel 2.98 mm inside diameter tubing (L/d=305) and a pressure of about 203 kPa. The outside diameter of the test section was 4.76-mm. CHF was found to decrease with a decrease in mass flux (mass fluxes varied between 50 to 200 kg/m^{2}s). CHF qualities were found to be relatively high, above 0.5 and increased with quality. The relative size of the channel compared to the wall thickness suggests that conduction may have played a role in the CHF condition in these studies. However, this was not analyzed.

Lezzi et al. [32] reported experimental results on CHF in forced convection boiling of water in a horizontal tube of diameter 1 mm and L/d=250, 500 and 1,000. The tube wall thickness was 0.25 mm. The mass flux varied between 800 and 2,700 kg/m^{2}s. In all the cases the quality at the outlet was high (greater than 0.6), and the critical heat flux was reached through dryout. They claimed that no oscillations affected the CHF condition, but did not substantiate this claim.

Convective boiling of R-123 and FC72 in 28-cm long horizontal stainless steel tubes of inner diameters of 0.19, 0.3 and 0.51 mm was investigated by Yen et al. [14]. The test section was heated by a direct current. For boiling, the heat transfer coefficients de-

creased with vapor quality up to x =0.3 and then remained constant until x =1, which suggests that the "traditional" CHF condition did not occur. The authors concluded that the heat transfer characteristics were caused by the size of the nucleating bubbles been limited by the confined space, because when the bubbles grew they immediately attached to the surrounding tube wall.

Recently, Wojtan et al. [33] investigated saturated critical heat flux in single uniformly heated microchannels of 0.5 mm and 0.8 mm internal diameters using R-134a and R-245fa. A valve was installed between the upstream temperature-controlled refrigerant storage vessel and the test section to avoid flow oscillations. However, the pressure drop oscillations during the boiling tests were not quantified. They did not find any influence of inlet subcooling on CHF, but at the same time they found the CHF to decrease with an increase in exit quality; however, the range of inlet subcooling considered was very limited ranging from 4.5°C to 12°C. They found that at the same mass flux, CHF increased with increasing diameter, which is the opposite of the effect found by Bergles et al. [27]. They presented a new correlation to predict CHF in circular uniformly heated microchannel.

Thus, there is no general agreement on the trends in the CHF condition in mini/microchannels so far. For example, in minichannels, Roach et al. [28] and Wojtan et al. [33] found the CHF to increase with increasing channel diameter but Bergles et al. [27] found an inverse dependence of diameter on CHF. Oh and Englert [29] found a weak linear relationship between inlet subcooling and CHF, but Bowers and Mudawar [15] and Wojtan et al [33] found that the CHF was not affected by the inlet subcooling. The data by Yu et al. [31] indicated that the CHF increased with an increase in exit quality, but the Wojtan et al. [33] data depicts the opposite effect. The CHF studies by Roach et al. [28] shows that the CHF increases with increasing pressure, but the data in some studies [33] do not show a strong dependence of pressure on CHF. Many researchers have attempted to predict their data with existing correlations, but with mixed results. Many different correlations have been developed, but they are mostly applicable to the limited data range over which the experiments were conducted. Conjugate heat transfer effects have been neglected, and the effect of flow instabilities have not been investigated properly during some of the experiments.

3. Experimental apparatus and procedures at Rensselaer

To avoid some of the problems (i.e., conjugate effects, parallel channel instabilities, two-phase flow instabilities in single tubes) associated with previous CHF experiments, we have designed and constructed an experiment to study CHF in thin-wall single stainless steel tubes (Roday et al. [18]). The test facility is shown in Fig. 5; the test section is shown in Fig. 6. Two items are of particular interest: the needle valve just upstream of the test section was used to impose a very large pressure drop (130-200 kPa), which eliminated two-phase flow instabilities; and the guard heater, which eliminated heat losses. The test sections were individual hypodermic tubes made of 304 stainless steel; their ends were sanded and polished to ensure that no burrs were present. T-Type thermocouples were mounted at six different locations on the test section for wall temperature measurements. Also, one thermocouple was mounted on the test section ahead of the heated length to check for any backflow of vapor and axial conduction away from the heated section. Degassed water (2.2 ppm oxygen content) was used as the working fluid. A wide range of pressures, mass fluxes, and inlet temperatures were used, and three different tubes were investigated: ID/OD (in mm) of 0.286/0.45, 0.427/0.55, and 0.7/0.9.

Single-phase experiments were first performed to check pressure measurements, the energy balance, and heat transfer performance. The ratio of the total experimental pressure drop (sum of the pressure drops at the entrance, in the developing flow region, fully developed region and the exit) to that calculated using correlations from the literature was within ± 6%. Energy balances generally were within ±5%. During the single-phase heat transfer experiments, the flow was hydrodynamically fully developed but was thermally developing through the length of the heated section.

The heat transfer results were compared with the modified Hausen correlation (for constant heat flux), which overpredicted the data by about 34 % at lower Reynolds number (Re~200) but underpredicted it by about 50% at Re~1200. However, these laminar single-phase heat transfer results were consistent with other results from the literature [34, 35]; no explanation has been offered yet as to why there is a different behavior compared to conventional size tubes.

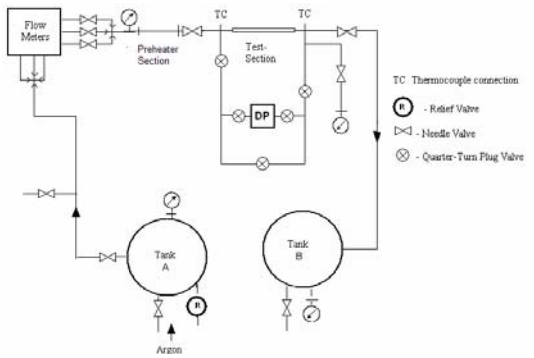

Fig. 5. Description of test facility of Roday et al. [18].

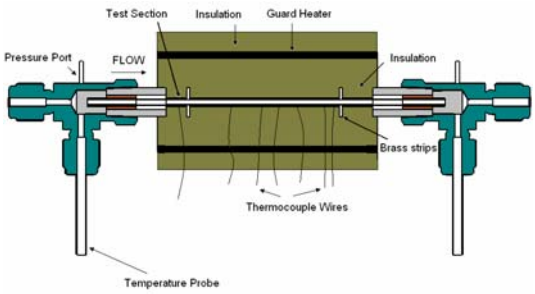

Fig. 6. Test-section assembly of Roday et al. [18]

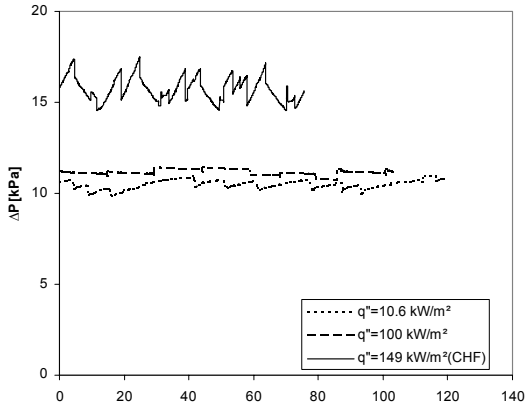

Fig. 7. Pressure drop versus time for d=0.427 mm, G=560 kgm^{2}s, ΔT_{sub}=38ºC, P_e= 25 kPa, [18].

Flow was stabilized during the CHF experiments by maintaining a very high pressure drop upstream of the test section. A thermocouple mounted on the test section wall just before the heated section did not show any variations in temperature, which indicated that there was no backflow of vapor or axial conduction outwards from the heated section. The pressure

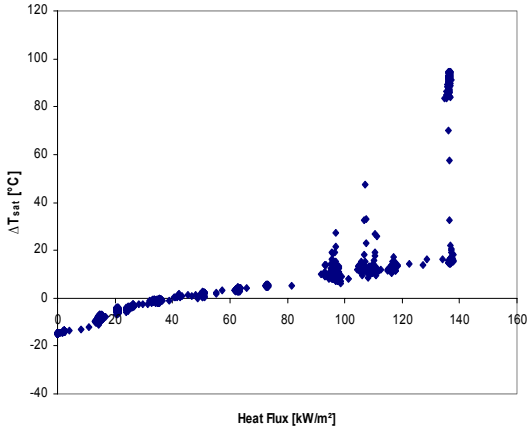

Fig. 8. Wall superheat versus heat flux (d=0.427 mm, P_e= 25 kPa; G=315 kg/m^{2}s; ΔT_{sub}=15°C) [18].

drop showed only small fluctuations with time (single- and two-phase flow regimes) except for very close to the CHF condition. One such plot of pressure drop versus time is shown in Fig. 7; the magnitude of the fluctuations was typical of all tests.

For these well-stabilized flow boiling tests we saw a variety of effects that were not necessarily consistent with results from the literature. Generally, there was a characteristic sharp rise in wall temperature at the point of CHF, as can be seen in the plot of wall superheat versus heat flux depicted in Fig. 8, with some jumping around in the wall temperature before reaching the CHF. Lazarek and Black [30] observed a similar wall temperature response during CHF tests in a 3.1 mm diameter tube at mass flux of about 270 kg/m^{2}s. Fig. 9 shows the wall temperatures at six locations along the length of the heated section for two different conditions. For the lower pressure data, the CHF condition occurred towards the exit of the tube at which point the wall temperatures were considerably higher compared to those closer to the inlet of the tube.

The characteristic CHF did not occur for some of the experiments up to high heat fluxes, at which point power was shut down so that the test sections were not destroyed. This happened for some tests at low values of inlet subcooling (ΔT_{sub}=2 – 7ºC). Fig. 10 shows the exit wall temperature variation with heat flux at an exit pressure of 102 kPa, and one axial temperature data set is also shown on Fig. 9. The wall temperature linearly increased with heat flux, but there was no sudden wall temperature spike as is normally associated with the CHF condition.

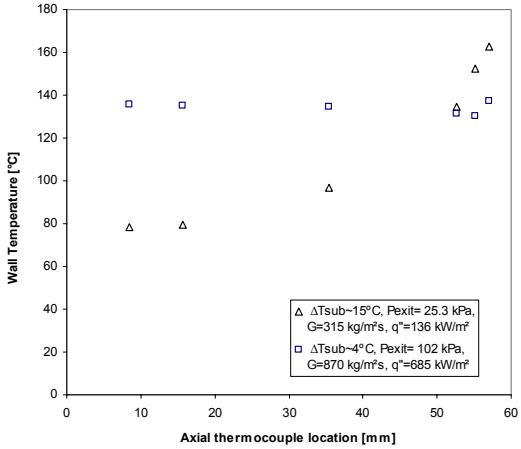

Fig. 9. Axial wall temperature variation (d=0.427mm) [18].

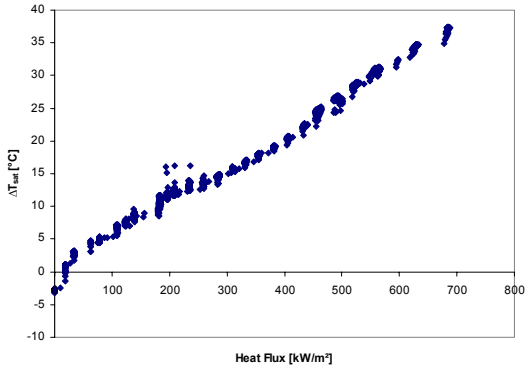

Fig. 10. Wall superheat versus heat flux (d=0.427 mm, P_e = 102 kPa; G=870 kg/m^{2}s; ΔT_{sub}~4°C) [18].

Other tests conducted for slightly lower mass fluxes (e.g., G= 560 kg/m^{2}s) showed the wall temperature to suddenly increase (by about 30°C) and fall back a few times during the experiment but no characteristic CHF was observed. It might be possible that the flow transitions to an "inverted annular" type even at lower heat flux levels, and boiling takes place through a stable vapor film. During this "film" type of boiling, the wall temperatures linearly increased as the heat flux was raised. More tests need to be conducted and further studies need to be done to confirm this phenomenon. Several other researchers have observed similar behavior (e.g., Roach et al. [28], Fukuyama and Hirata [36], Hosaka et al. [37]).

Additional data from our lab [18] and some new data are presented below in the discussion of parametric trends in the CHF condition.

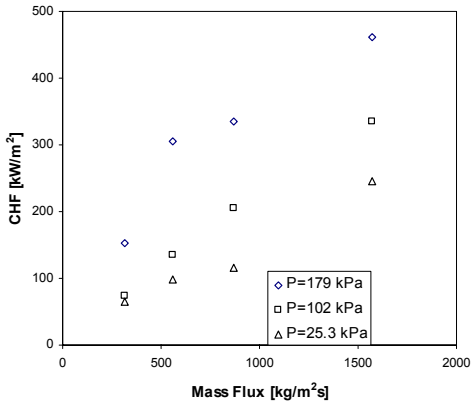

Fig. 11. Effect of Mass Flux on CHF for water, ΔT_{sub} ~ 46°C, L=59 mm, d=0.427 mm [18].

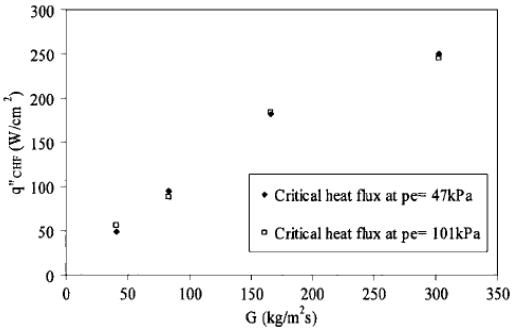

Fig. 12. Critical heat flux dependence on G for water d_h=0.227 mm, L=10 mm (Kosar et al. [38]).

4. Parametric effects on CHF

4.1 Effect of Mass flux on CHF

Fig. 11 depicts the dependence of CHF on mass flux for the three exit pressures with inlet subcooling, ΔT_{sub} ~ 46°C; the subcooled CHF condition was observed in these data. The CHF increases with an increase in mass flux. The CHF increases with an increase in exit pressure for the same value of mass flux; the slope of the CHF–G curves increases with pressure. A similar observation was made at other values of inlet subcooling.

A similar mass flux dependence of CHF has been observed by other researchers and is depicted in Fig. 12 for water at reduced pressures through parallel microchannels of 0.227 mm hydraulic diameter (Koşar et al. [38]), and Fig. 13 shows data for flow of R-134a through a single stainless steel tube of 0.5 mm and 0.8 mm inside diameter (Wojtan et al. [33]). Thus,

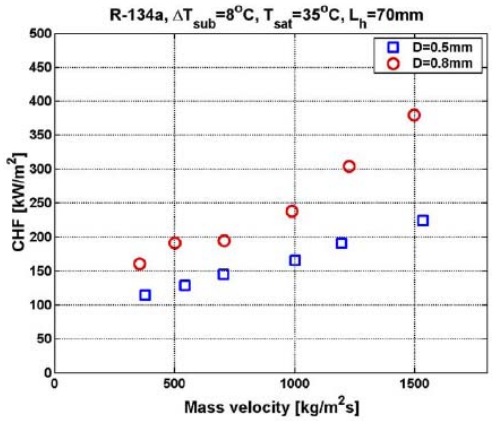

Fig. 13. Mass flux dependence on CHF for R-134a (Wojtan et al. [33]).

an increasing CHF with mass flux is seen in studies with different fluids. However, note that the water data of Kosar et al. [38] and Roday et al. [18] have two significant differences. The Kosar et al. data have significantly higher CHFs—perhaps due to a smaller hydraulic diameter or conjugate effects—and do not show any pressure dependence, unlike the large pressure dependency shown by the Roday et al. data.

The study conducted by Koşar and Peles [20] for R-123 in silicon-based microchannels also show the CHF to increase with increase in mass flux, but their data show some dependence on pressure, and the slope of the curves vary with pressure (Fig. 14) similar to the data of Roday et al. [18] in Fig. 11 and Wojtan et al. [33] in Fig. 13, but unlike the data by Kosar et al. [38] in Fig. 12. Maximum slope was obtained when the system pressure was maintained at 315 kPa, and CHF values were greater than for the four other pressures.

4.2 Effect of inlet subcooling

The effect of inlet subcooling on CHF is shown in Fig. 15 for all exit pressures for two mass fluxes [18]. For the higher mass flux, at higher levels of inlet subcooling, CHF slightly decreased with a decrease in inlet subcooling. But at lower subcoolings (water inlet temperature close to the saturation temperature), the CHF increased with a decrease in subcooling. The same trend was observed at the three different pressures; the value of CHF was higher for the higher exit pressure. A similar behavior was observed for the lower mass flux as well. For the cases where the CHF dramatically increased with reduction in inlet subcooling, the exit quality at CHF was close to zero.

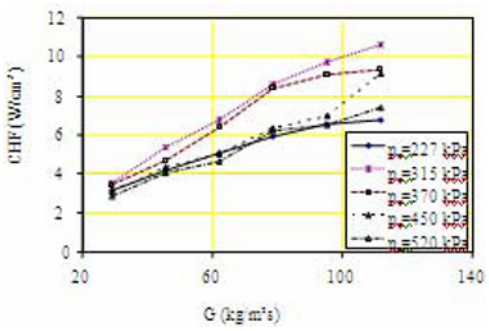

Fig. 14. Critical heat flux dependence on G in R-123 with d_h=0.227 mm, L=10 mm (Kosar and Peles [20]).

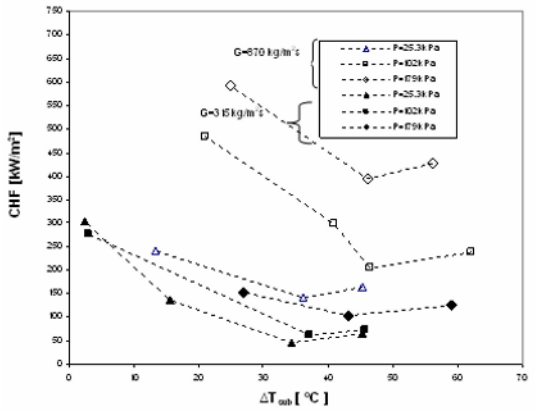

Fig. 15. Effect of Inlet Subcooling on CHF for water, d=0.427 mm, L=59 mm [18].

These data are not in agreement with some other data that exist for CHF in microchannels. For example, the data by Wojtan et al. [33] show the CHF to be affected by exit quality, but only a small influence of inlet subcooling is observed as shown in Fig. 16. However, they state that measurements with larger inlet subcoolings were not possible, and so the data depicted in Fig. 16 are for subcooling ranging only from 4.5°C to 12°C. They claim the observation to be in good agreement with the results of Qu and Mudawar [16] for parallel microchannels.

Qu and Mudawar [16] observed parallel channel instability (vapor back flow) as the CHF was approached, resulting in a diminished influence of inlet subcooling as vapor mixed with the subcooled inlet fluid in the plenum (Fig. 2). Their data showed hardly any influence of inlet subcooling as is seen in Fig. 17. They found this unique to parallel microchannels because instabilities occurred much more in parallel

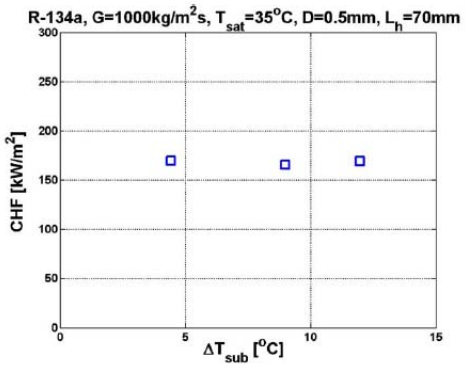

Fig. 16. Effect of inlet subcooling on CHF (Wojtan et al. [33]).

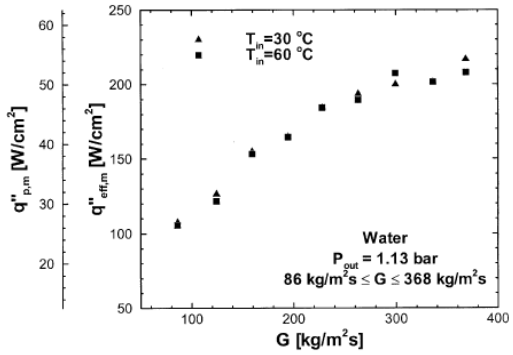

Fig. 17. Inlet subcooling effect on CHF for water d_h=0.34 mm (Qu and Mudawar [16]).

microchannels than in single tubes, but at lower subcoolings (water inlet temperature close to the saturation temperature), the CHF increased with a decrease in subcooling.

4.3 Effect of exit quality on CHF

Detailed results for the effect of exit quality on CHF [18] are presented in Fig. 18. Note that the CHF first decreases with an increase in quality in the subcooled region, but with a further increase in quality (near zero quality and above), the CHF is found to increase with quality. Much higher values of CHF are found in the region close to saturation when compared to the high subcooled region. With still further increases in heat flux/exit quality, the CHF condition did not occur even when the wall superheat (ΔT_{sat}= T_w-T_{sat}) reached about 40-60°C; the wall temperature increased essentially linearly with increases in heat flux (Fig. 10). At this point, the experiment was terminated to save the test section. Such data points

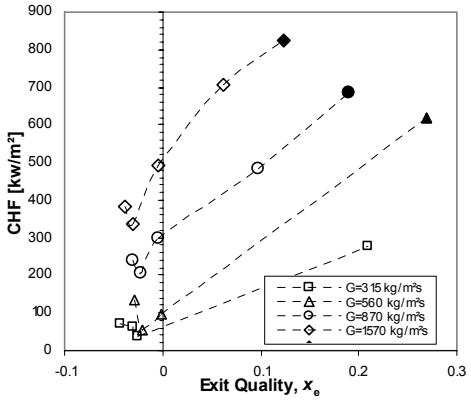

Fig. 18. Variation of CHF with quality for d=0.427 mm, L=59 mm, P_e= 102 kPa (abs) (solid marker indicates that experiment was stopped before CHF was observed) [18].

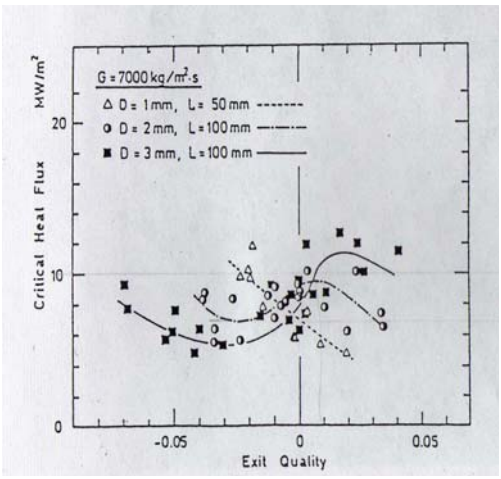

Fig. 19. Effect of exit quality on CHF for water near saturated region (Nariai et al. [26]).

where CHF did not occur are indicated by solid markers in Fig. 18. Similar results were obtained at 25 and 179 kPa.

The increase in CHF from the subcooled to the saturated region can be attributed to the void fraction change. In such a small diameter tube, the void fraction becomes significant enough to cause an increase in the flow velocity, thereby causing an increase in the value of CHF. Similar trends were observed at studies conducted at the two other exit pressures. Nariai et al [26] reported a similar observation in their studies on CHF in minitubes (1mm-3mm inside diameter) but with much higher mass fluxes (7000-11,000 kg/m^{2}s) as depicted in Fig. 19 .The maximum exit quality in their data was 0.05. Bergles et al. [27]

reported similar findings for flow of water through a 2.38 mm tube with a mass flux of 3000 kg/m^{2}s.

This behavior is different from the observations of Wojtan et al. [33], who found the CHF to decrease with an increase in quality as depicted in Fig. 20. However, the mass fluxes were not specified, and each datapoint is possibly at a different mass flux. Studies by Koşar and Peles [20] suggests that the exit mass quality at the CHF condition decreases with increasing mass velocity at fixed pressure as seen in Fig. 21, but the effect of quality at a constant mass flux is not specified.

For tests conducted with the 0.286 mm tube [39], very high qualities at CHF were observed. Also, the CHF was found to increase with the increase in exit quality. These data were compared with the results of Yu et al. [31] who had conducted CHF studies in a 2.98 mm diameter tube.

As seen from Fig. 22, the results are qualitatively similar. The CHF values in this study [39] are much higher with a tube of diameter about 1/10th that of Yu et al.

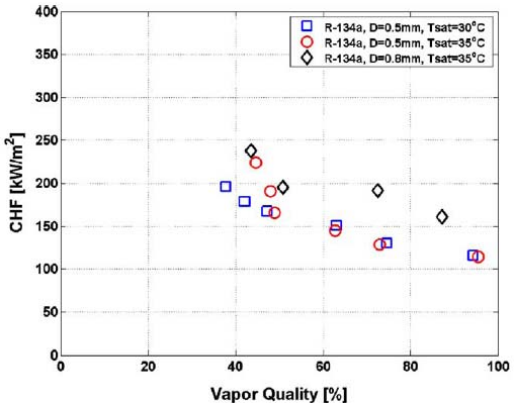

Fig. 20. Variation of CHF with exit quality for R-134a [33].

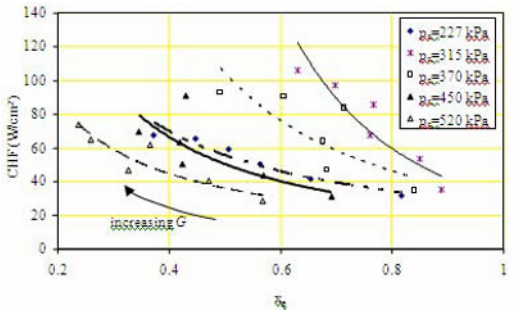

Fig. 21. CHF dependence on quality for R-123 with d_{hyd}= 0.227 mm, L=10 mm [20].

Further CHF studies [40] were conducted with water for tube inside diameters of 0.286 mm, 0.427 mm and 0.700 mm for pressures from sub-atmospheric (25 kPa) to above atmospheric pressure (179 kPa) for different L/d ratios (75–200) and all the water CHF data were mapped using available flow-pattern maps for microchannels. The CHF data when mapped using the flow pattern map of Hassan et al. [41] are shown in Fig. 23. It is seen from this figure that most of the data fall in the churn flow, churn-annular transition or annular flow very close to the transition zone. The churn flow is characterized by a highly irregular interface with oscillatory flow of the liquid. With increase in quality in the saturated region, more vapor is generated, and it is possible that the waves are stabilized due to the high vapor. This might be a possible reason for increase in CHF with quality during the transition as observed in all the saturated CHF data for the tube diameters of 0.427 mm and 0.700 mm. Some of the data for tube diameter of 0.286 mm were in the annular flow, with the remaining in churn or churn-annular regime. For all data points (in churn flow as well as churn-annular transition) and even those in annular flow closer to transition, the flow might still be oscillatory and a similar behavior as observed in other tube diameters is expected where the CHF increases with quality. For tube of 0.286 mm diameter, annular flow far away from transition is observed at very high qualities where we would expect behavior similar to conventional tubes (CHF decreasing with quality).

Revellin and Thome [42] have proposed a new flow-map for evaporating flow in microchannels based on flow visualization. It classifies the flow into three regimes–isolated bubble regime, coalescing

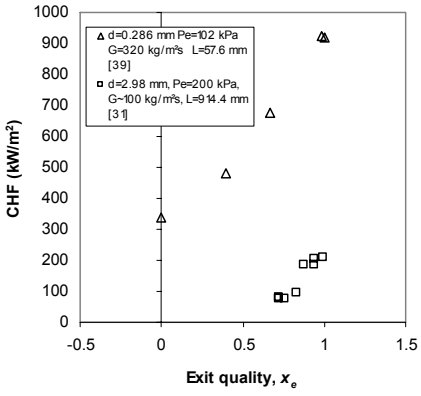

Fig. 22. Comparison of exit quality on CHF for d=0.286 mm [39], and d=2.98 mm [31].

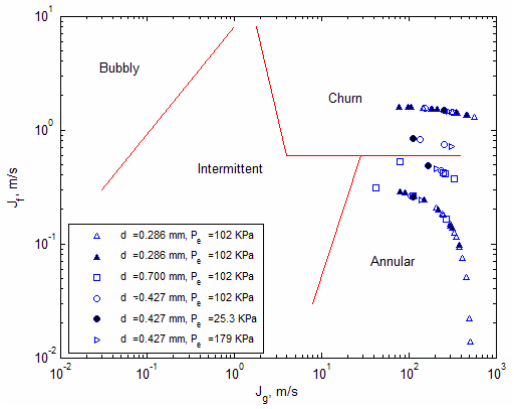

Fig. 23. Water data flow patterns using flow-pattern map of Hassan et al. [41].

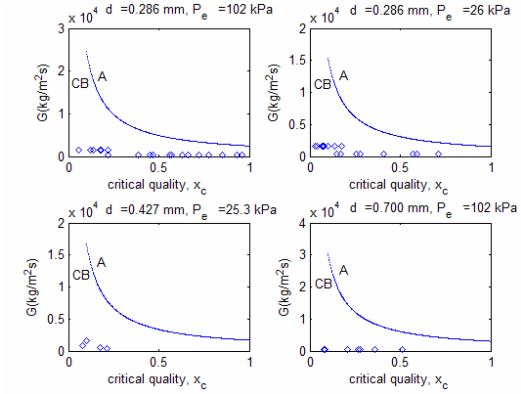

Fig. 24. Water CHF data mapped using flow pattern map of Revellin and Thome [42].

bubble regime and the annular regime. This flow map is not universal. A new flow map is needed for every diameter, pressure and heat flux. Revellin and Thome flow map showing only the transition from coalescing bubble region to annular region is used to map the water CHF data from [40] otherwise a new flow map would be needed for each CHF data point

In Fig. 24, the solid lines indicate the flow pattern transitions from coalescing bubble (CB) to annular flow (A) regime using Revellin and Thome correlation and the symbols indicate the experimental CHF data points. This flow-map predicts that none of the CHF data points are in the annular region and data points for tube diameters of 0.7 mm and 0.427 mm are far away from the transition line. However, the Hassan et al. flow map predicts annular flow for some of the experimental CHF data points. Again, it should be noted that the experimental parameters in the CHF studies with water are very different from those that are used to obtain the Revellin and Thome flow map.

Thus, based on the conclusions drawn from the data and the flow regime map, the behavior of CHF with quality can be summarized in the Fig. 25 in which the behavior of CHF with quality is marked by two transition points: Transition A, which might depend on the point of net vapor generation, and Transition B, which depends on the establishment of annular flow in the tube. These transition points are clearly functions of the operating parameters, and based on the chosen condition, one or the other type of behavior is seen. The CHF condition between these two transition points is governed by a transitional behavior as the mechanism changes from (probably) a DNB-type behavior in the subcooled region to a dry

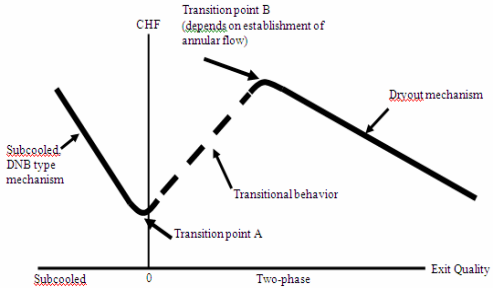

Fig. 25. Speculations on the trends of CHF with exit quality.

out behavior at higher qualities.

4.4 Effect of tube diameter on CHF

New data for the three different tube diameters are given in Fig. 26. The data compared are for a mass flux of about 320 kg/m^{2}s, $L_h/d \approx 140$, and exit pressure close to atmospheric. The CHF increased substantially with a reduction in tube diameter to 0.286 mm from 0.427 mm. The differences in the CHF values for tube diameters of 0.427 mm and 0.7 mm are not substantial. We see a similar large increase in CHF between the 0.227 mm data of Koşar et al. [38] (Fig. 12) and the 0.427 mm diameter data of Roday et al. [18] (Fig. 11) as well as the very large increase in CHF going from d=2.98 mm to d=0.286 mm shown in Fig. 22. Based on these data, there may be some sort of transition in the range of $d \approx 0.5$ mm, wherein below this diameter the CHF is increased significantly and above this value, diameter has a weaker effect on the CHF condition. A similar inverse relationship of CHF on diameter was observed by Ber-

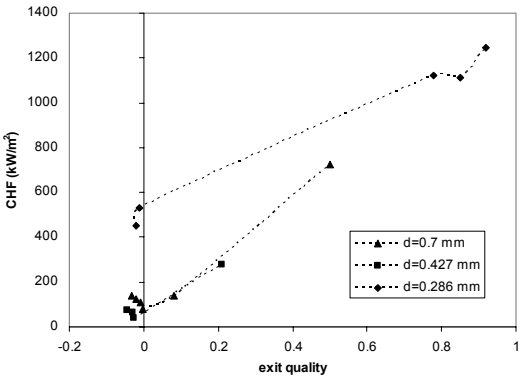

Fig. 26. Effect of tube diameter on CHF, L/d=139, G~320 kg/m^{2}s, P_e≈102 kPa [18].

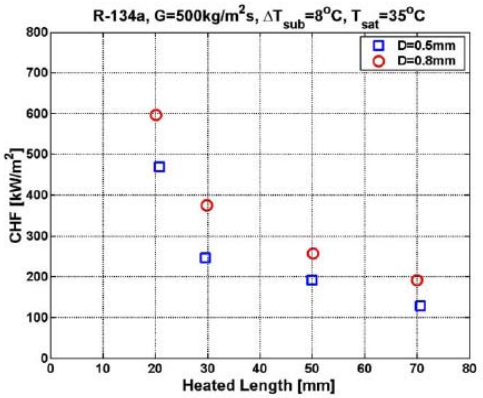

Fig. 27. Variation of CHF with heated length (Wojtan et al. [33]).

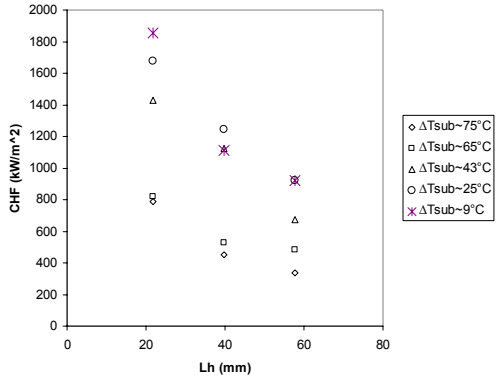

Fig. 28. Effect of heated length on CHF (d=0.286 mm G=320 kg/m^{2}s) [39].

gles et al. [27]. However, as seen in Fig. 27, the data by Wojtan et al. [33] for refrigerants do not depict the inverse dependence of CHF on diameter.

4.5 Effect of heated length on CHF

New data were obtained for the two diameters of 0.286 mm and 0.7 mm over different L_h/d ratios. For both tube diameters, the CHF decreased with an increase in heated length. The data for d=0.286 mm [39] are depicted in Fig. 28. Research conducted by Wojtan et al. [33] shows agreement with this as is seen in Fig. 27.

5. CHF models and comparison of data with existing correlations

There have been attempts to model the CHF condition, and different trigger mechanisms for CHF have been proposed. Weisman [43] provided a comprehensive review of the theoretically based approaches to predict the CHF condition in conventional size tubes. An earlier model for predicting CHF for subcooled flows, as described by Tong and Tang [44], was based on boundary layer separation, coupled with subcooled core liquid exchange and interface condensation. For highly subcooled flows, Weisman et al. [45] suggested that the critical void fraction in the bubble layer triggered the CHF mechanism. Based on flow visualization, Lee and Mudawar [46] proposed that CHF in low-quality flows occurred when the liquid sublayer that separated vapor blankets from the wall was disrupted. The Katto [47] and Celata et al. [48] models for CHF are similar to Lee and Mudawar model; the difference lies in the method used to calculate vapor velocity and liquid sublayer thickness. The fourth CHF mechanism, based on lift-off of the liquid-vapor interface at the initiation of CHF, was proposed by Galloway and Mudawar's [49] extensive flow visualization experiments carried out at near saturated conditions and relatively low flow velocities. CHF in high-quality flows was due to liquid dryout in the annular regime, initiated by the imbalance between droplet entrainment and deposition. Dryout models such as by Hewitt et al. [50] and Sugawara [51] utilize empirical correlations for entrainment and deposition.

In studies by Thome et al. [52] in microchannels, with the aid of a high-speed camera (Fig. 29) the bubbly flow regime (bubbles smaller than the channel size) lifespan is short, the bubbles grow to the channel size very quickly and the dominant flow regime is the elongated bubble flow regime. Evaporation occurs at the moving contact line of the expanding vapor slug

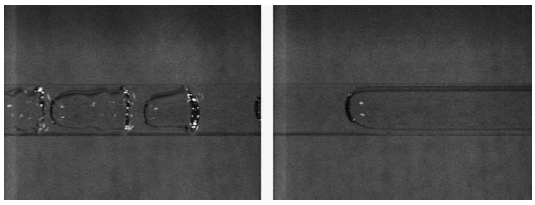

Fig. 29. Video image of an elongated bubble in a glass tube of 0.8 mm diameter [52].

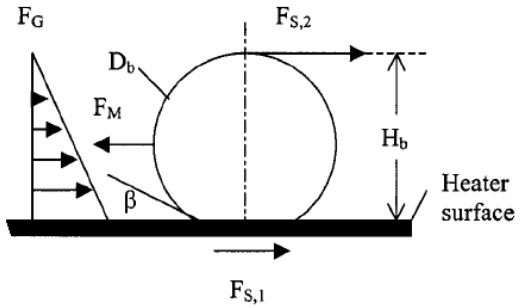

Fig. 30. Forces acting on a bubble; pool boiling model-Kandlikar [53].

as well as over the channel wall which is covered with a thin liquid film between the wall and the vapor slug. The complete evaporation of this liquid film initiates dryout.

The contact angle is believed to play an important role during dryout and rewetting phenomena in microchannels. Few of the flow boiling CHF models available in the literature for conventional size channels explicitly consider the effect of contact angle on the CHF mechanism, which probably plays a stronger role in microchannels than conventional size channels.

The first attempt to include the effect of contact angle was made by Kandlikar [53] to predict the CHF during pool boiling. He considered a force balance on the bubble attached to a horizontal surface, as shown in Fig. 30. At high evaporation rates near CHF, the force due to change in momentum (F_M) as a result of evaporation becomes larger than the sum of the gravitational (F_G) and surface tension forces ($F_{S,1}$ and $F_{,S,2}$) holding the bubble in place and this results in the liquid-vapor interface to move along the heater surface leading to the CHF condition.

In a flow boiling situation and based on these forces acting on a liquid-vapor interface, Kuan and Kandlikar [21] proposed a theoretical model for CHF considering the effect of the contact angle. The critical heat flux was expressed as

$$q''_{CHF} = Ch_{fg}\sqrt{\rho_g}\left(\sqrt{\frac{2\sigma\cos\theta}{b}+\frac{G^2}{2\bar{\rho}}}\right) \quad (2)$$

where b is the channel height and ρ is the average density based on the mass quality. The single constant C, which relates the interfacial area based heat flux to the CHF based on channel-wall surface area, was determined from experimental data. Thus, this model cannot be validated until a large number of CHF data in microchannels become available. No attempt was made to investigate the agreement with some of the existing microchannel CHF data.

Revellin and Thome [54] developed a theoretical model to predict CHF for flow of refrigerants in circular microchannels based on solving the conservation of mass and momentum equations along with the Laplace-Young equation and includes the effect of the interfacial waves during annular flow. In this model, dryout occurs when the height of the interfacial wave becomes equal to the calculated film thickness. The constants in the expression for calculating the height of the interfacial wave are based on the data from Wojtan et al. [33] and Lazarek and Black [30]. The axial or radial conduction effects are neglected in this model and the inlet flow is assumed to be a saturated liquid. Also, this model assumes no entrainment during annular flow. The model was compared with the CHF data from Wojtan et al. and Lazarek and Black (data from which constants in the expression were derived) and it was found that more than 96% of the data are predicted within ±20% error with a mean absolute error of 8%. When the parametric sensitivities of the model were studied, it was found that the CHF increases with an increase in diameter of the tube. This is contradictory to some other studies that have been conducted to study CHF in microchannels.

The other approach to understand the CHF in relation to the system variables is of an empirical nature where a relationship between CHF and the system variables is developed without a detailed understanding on the mechanisms leading to the CHF condition. As mentioned earlier, various correlations have been proposed but generally are applicable to limited database ranges. Nevertheless, the CHF data obtained at Rensselaer, for the exit at about atmospheric pressure were compared with these correlations for two different tube diameters of 0.286 mm and 0.427 mm [39]. The CHF data in the subcooled region were compared

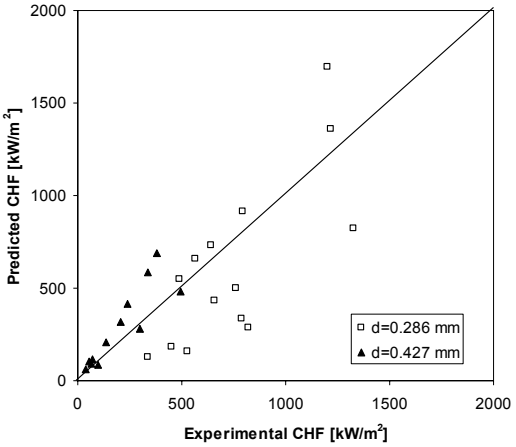

Fig. 31. Comparison of CHF data [39] with subcooled CHF correlation of Hall and Mudawar [55].

with the Hall and Mudawar correlation [55]. This is represented in Fig. 31. Some of the deviation is because the Hall and Mudawar correlation overpredicts the data at very high inlet subcoolings and does not take into the increased CHF behavior seen as the qualities approach zero.

As mentioned previously, further CHF studies were conducted at Rensselaer for flow boiling of water through microtubes [40] and the data did not compare well with the Hall and Mudawar correlation for subcooled flow. A new subcooled CHF correlation [40] was developed for low mass fluxes. The correlation is expressed as

$$Bo = \frac{C_1 We_d^{C_2} \cdot \left(\frac{\rho_f}{\rho_g}\right)^{C_3} \left(\frac{L_h}{d}\right)^{C_4} \left(\frac{\Delta h_i}{h_{fg}} + C_5\right)}{\left(We_d + C_6\right)\left(\frac{L_h}{d} + C_7\right)} \quad (3)$$

and the constants in the correlation are tabulated below:

For most of the subcooled data, the CHF first decreases with increase in exit quality and it is speculated that beyond PNVG (point of net vapour generation) the CHF has an increasing trend with quality [40]. Those data points which show the decreasing trend for $x < x_{PNVG}$ have been used for developing the correlation

The comparison of the predicted Boiling number (from the correlation in Eq. 2) with the experimental boiling number for the subcooled CHF data is shown

Table 1. Values of the constants in the proposed correlation.

C_1	44587	C_6	-0.425
C_2	1.136	C_7	-279.8
C_3	-0.625		
C_4	-1.680		
C_5	-0.0157		

Table 2. Non-dimensional parametric range for establishing the correlation.

Parameter	Range
Weber Number, We_d	0.46– 20.01
Density ratio, ρ_f/ρ_g	930 – 6022
Length-to-diameter ratio, L_h/d	75 – 200
Inlet subcooling/Enthalpy ratio, $\Delta h_i/h_{fg}$	-0.149 – -0.053

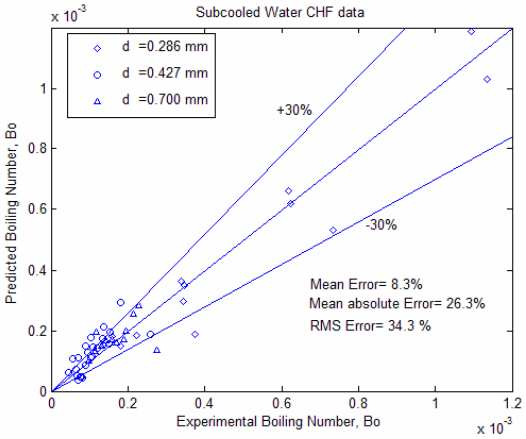

Fig. 32. Comparison of experimental water CHF data with the correlation from Eq. (1) [40].

in Fig. 32. It can be seen that the correlation predicts the data reasonably well, with RMS error of 34.3%.

All the subcooled CHF data available in the literature are for very high mass fluxes and pressures such as [23, 24, 56] and, hence, cannot be compared with the new correlation. Bergles et al. [57] have CHF data at relatively lower mass fluxes of about 3000 kg/m^{2}s, but the inlet conditions (temperature or enthalpy) are not provided and, hence, the data cannot be compared with the proposed correlation.

Very few CHF data points could be obtained in the saturated region, because the wall temperatures kept on linearly increasing with heat flux, and very high wall superheats were obtained even at significantly lower exit qualities. For most of the tests in the satu-

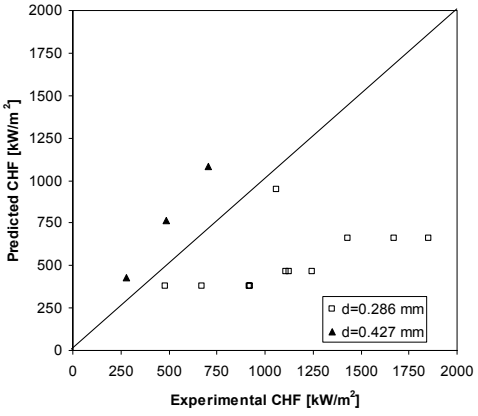

Fig. 33. Comparison of CHF data [39] with saturated CHF correlation of Qu and Mudawar [16].

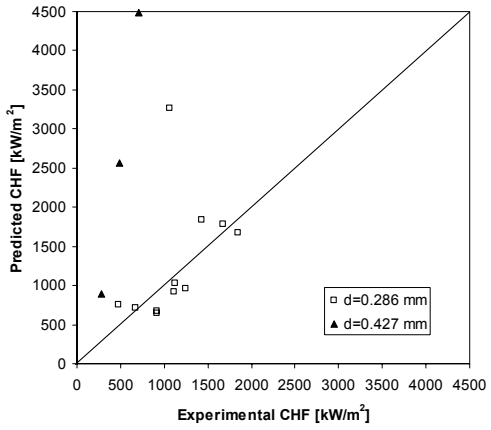

Fig. 34. Comparison of CHF data [39] with saturated CHF correlation of Zhang et al. [58].

rated region, the characteristic CHF was not observed and the experiment had to be terminated to save the test section. For the saturated CHF data in study [39], two of the correlations developed for mini/microchannels were considered for comparison: Qu and Mudawar [16], and Zhang et al. [58]. Zhang et al. [58] evaluated existing correlations for flow boiling of water with available databases from small diameter tubes and developed a new correlation based on the inlet conditions by performing parametric trend analysis of the collected database.

The correlation from [16] does not consider the effect of inlet subcooling. However, the data presented in this study clearly shows an effect of inlet subcooling on CHF. The comparisons of the saturated CHF data with the Qu and Mudawar and Zhang et al. correlations are shown in Fig. 33 and Fig. 34, respectively. The Zhang correlation highly overpredicts the data for d=0.427 mm. It might be because this correlation was developed by using an existing database with very few small diameter data, and those data are almost all in the high mass flux range. The Qu and Mudawar correlation also does not predict the data well for either tube diameter as it does not take into account the inlet subcooling effect.

6. Conclusions

The current available literature on CHF in microchannels is reviewed and recent data are presented. The following conclusions can be drawn:

There are inconsistencies in the experimental CHF results—disagreements on the influence of inlet subcooling, pressure, exit quality and diameter on CHF.

The CHF is found to increase with an increase in mass flux and decrease with an increase in heated length. In most studies, CHF is found to decrease with an increase in diameter. The effect of quality is not well understood. Both increases and decreases of CHF with quality have been observed. In the research carried out at Rensselaer, a more complex behaviour of CHF with quality is seen and the possible reasons for such a behavior have been investigated in detail.

Most of the CHF data in parallel microchannels are influenced by flow instabilities and conjugate effects. No attempt has been made to analyze conjugate effects experimentally.

Data compared with existing microchannel correlations shows mixed results. This is because most of the correlations are applicable to the limited data range over which the experiments were conducted. A new subcooled CHF correlation for low flow rates is presented in this study.

There are only two CHF models that exist for flow boiling in microchannels. One of the models, that by Revellin and Thome, has been compared with the limited experimental data. The effect of contact angle and conjugate effects due to the wall should be incorporated in the CHF model

Based on this review, we believe that the following studies need to be undertaken to provide a better understanding of the CHF condition in microchannels:

More data with different fluids for a variety parameters—diameter, mass flux, pressure, subcooling—need to be obtained under stable flow conditions.

Flow instabilities need to be addressed and quantified.

The effect of conjugate heat transfer effects should be studied to determine its effects on the CHF condition.

Phenomenological model for flow boiling CHF should be developed which will include the effects of the contact angle and also the conjugate heat transfer

Satisfactory CHF correlations need to be developed which will encompass different operating conditions.

Acknowledgment

This research was supported by the National Science Foundation (NSF) under Grant Number CTS-0245642, and by the Office of Naval Research as a MURI award (prime award number N00014-07-1-0723). Graduate student support from the Department of Mechanical, Aerospace and Nuclear Engineering at Rensselaer Polytechnic Institute is also gratefully acknowledged.

References

[1] G. Moore, Cramming more components onto integrated circuits, *Electronics,* 38 (8) 114-117, 1965.

[2] R. J. Hannemann, Thermal control of electronics: perspectives and prospects, *Rohsenow Symposium on Future Trends in Heat Transfer*, Warren M. Rohsenow Heat and Mass Transfer Laboratory, Massachusetts Institute of Technology, Cambridge, MA, 2003.

[3] D. B. Tuckerman and R. F. W. Pease, High-Performance heat sinking for VLSI, *IEEE Electron Devices Letters*, vol. EDL-2, 126-129, 1981.

[4] S. Kakac and H. Liu, Heat exchangers: Selection, rating and thermal design, *CRCPress*, 903-904, Chapter 9, 1998.

[5] S. G. Kandlikar and W. J. Grande, Evolution of microchannel flow Passages — Thermohydraulic Performance and Fabrication Technology," *Heat Transfer Engineering*, vol. 24, no. 1, pp. 3-17, 2003.

[6] A. E. Bergles, Burnout in boiling heat transfer: High-quality forced-convection systems, *Two-Phase Flow and Heat Transfer, China-U.S. Progress*, Hemisphere Publishing Corporation, New York, 177-206, 1985.

[7] B. Thompson and R. V. Macbeth, Boiling water heat transfer-Burnout in uniformly heated round tubes: A compilation of world data with accurate correlations, *Atomic Energy Establishment of Winfrith, AEEW-R356*, Winfrith, U.K., 1964.

[8] R. W. Bowring, A simple but accurate round tube uniform heat flux dryout Correlation over the pressure range 0.7-17 MN/m^2 (100-2500 psia), *Atomic Energy Establishment of Winfrith, AEEW- R789*, Winfrith, U.K., 1972.

[9] Heat and Mass Transfer Section, Scientific Council, USSR Academy of Sciences, Tabular data for calculating burnout when boiling in uniformly heated round tubes, *Thermal Eng. (USSR)*, English transl., 23 (9) (1976) 90-92.

[10] Katto, Y. and Ohno, H., "An improved version of the generalized correlation of critical heat flux for the forced convective boiling in uniformly heat vertical tubes, *International Journal of Heat and Mass Transfer*, 27 (1984) 1641-1648.

[11] D. C. Groneveld, S. C. Cheng and T. Doan, 1986 AECL-UO critical heat flux lookup table, *Heat Transfer Engineering*, 7 (1986) 46-62.

[12] D. D. Hall and I. Mudawar, Critical heat flux (CHF) for water flow in tubes - I. Compilation and assessment of world CHF data, *International Journal of Heat and Mass Transfer*, 43 (14) (2000) 2573-2604.

[13] L. Jiang, M. Wong and Y. Zohar, Phase change in microchannel heat sink under forced convection boiling, *Proceedings of the IEEE Micro Electro Mechanical Systems (MEMS)*, 397-402, 2000.

[14] T. Yen, N. Kasagi and Y. Suzuki, Forced convective boiling heat transfer in microtubes at low mass and heat fluxes, *International Journal of Multiphase Flow*, 29 (2003) 1771-1792.

[15] M. B. Bowers and I. Mudawar, High flux boiling in low flow rate, low pressure drop mini-channel and micro-channel heat sinks," *International Journal of Heat and Mass Transfer*, 37 (2) 321-332, 1994.

[16] W. Qu and I. Mudawar, Measurement and correlation of critical heat flux in two-phase micro-channel heat sinks," *International Journal of Heat and Mass Transfer*, 47 (2004) 2045-2059.

[17] A. E. Bergles and S. G. Kandlikar, On the nature of critical heat flux in microchannels, *Journal of Heat Transfer*, 127 (2005) 101-107.

[18] A. P. Roday, T. Borca-Tasçiuc and M. K. Jensen, The Critical Heat Flux Condition with water in a uniformly heated microtube, *Journal of Heat Transfer*, 130, 2008.

[19] A. Koşar, C.-J. Kuo and Y. Peles, Suppression of boiling flow oscillations in parallel microchannels by inlet restrictors, *Journal of Heat Transfer*, 128 (2006) 251-260.

[20] A. Koşar and Y. Peles, Critical heat flux of R-123 in silicon-based microchannels, *Journal of Heat Transfer*,

2007, 129 (7) 844-851.

[21] W. K. Kuan and S. G. Kandlikar, Critical heat flux measurement and model for Refrigerant-123 under stabilized flow conditions in microchannels, *Proceedings of IMECE 2006, 2006 ASME International Mechanical Engineering Congress and Exposition, November 5-10, 2006, Chicago, Illinois, USA*, IMECE2006-13310.

[22] A. A. Rostami, A. Y. Hassan and S. L. Chia, Conjugate heat transfer in microchannels, *Heat Transfer and Transport Phenomena in Microsystems*, Banff, Alberta, Canada, 121-128, October 2000.

[23] C. L. Vandervort, A. E. Bergles and M. K. Jensen, An experimental study of critical heat flux in very high heat flux subcooled boiling, *International Journal of Heat and Mass Transfer*, 37 (1) (1994) 161-173.

[24] G. P. Celata, M. Cumo and A. Mariani, Burnout in highly subcooled water flow boiling in small diameter tubes, *International Journal of Heat and Mass Transfer*, 36 (5) (1993) 1269-1285.

[25] G. P. Celata, M. Cumo and A. Mariani, Geometrical effects on the subcooled flow boiling critical heat flux," *Revue Générale de Thermique*, 36 (1997) 807-814.

[26] H. Nariai, F. Inasaka and K. Uehara, Critical heat flux in narrow tubes with uniform heating, *Transactions of the Japanese Society of Mechanical Engineers*, 54 (502) 1406-1410, 1988.

[27] A. E. Bergles and W. M. Rohsenow, Forced-convection surface-boiling heat transfer and burnout in tubes of small diameter, *Contract AF 19 (604)-7344 Report, Department of Mechanical Engineering, Massachusetts Institute of Technology*, 1962.

[28] Roach, Jr., G. M., S. I. Abdel-Khalik, S. M. Ghiaasiaan, M. F. Dowling and S. M. Jeter, Low flow critical heat flux in heated microchannels, *Nuclear Science and Engineering*, 131 (1999) 411-425.

[29] C. H. Oh and S. B. Englert, Critical heat flux for low flow boiling in vertical uniformly heated thin rectangular channels, *International Journal of Heat and Mass Transfer*, 36(2) (1993) 325-335.

[30] G. M. Lazarek and S. H. Black, Evaporative heat transfer, pressure drop and critical heat flux in a small vertical tube with R-113," *International Journal of Heat and Mass Transfer*, 25 (7) (1982) 945-960.

[31] W. Yu, M. W. Wambsganss, J. R. Hull and D. M. France, Critical heat flux and Boiling Heat Transfer to Water in a 3–mm–diameter Horizontal Tube, *Proceedings of the 2001 Vehicle Thermal Management Systems Conference*, Paper No. 2001-01-1768, 2001.

[32] A. M. Lezzi, A. Niro and G. P. Beretta, Experimental data on CHF for forced convection water boiling in long horizontal capillary tubes, *Proceedings of the Tenth International Heat Transfer Conference,* Rugby, UK, 7 (1994) 491-496.

[33] L. Wojtan, R. Revellin and J. R. Thome, Investigation of saturated critical heat flux in a single uniformly heated microchannel, *Experimental Thermal and Fluid Science*, 30 (2006) 765-774.

[34] G. P. Celata, M. Cumo, M. Guglielmi and G. Zummo, Experimental investigation of hydraulic and single-phase heat transfer in 0.13–mm capillary tube, *Microscale Thermophysical Engineering*, 6 (2002) 85-97.

[35] X. F. Peng and G. P. Peterson, Convective heat transfer and flow friction for water flow in micro channel structures, *International Journal of Heat and Mass Transfer*, 39 (1996) 2599- 2608.

[36] Y. Fukuyama and H. Hirata, Boiling heat transfer characteristics with high mass flux and disappearance of CHF following to DNB, *Proceedings of the 7th International Heat Transfer Conference*, Hemisphere Publishing, Washington, D.C., 4 (1982) 273-278.

[37] H. Hosaka, M. Mirata and N. Kasagi, Forced convective subcooled boiling heat transfer and CHF in small diameter tubes, *Proceedings of the 9th International Heat Transfer Conference*, He misphere Publishing, Washington, D.C., 2 (1990) 129-134.

[38] A. Koşar, C. -J. Kuo and Y. Peles, Reduced pressure boiling heat transfer in rectangular microchannels with interconnected reentrant cavities," *Journal of Heat Transfer*, 127 (2005), pp. 1106-1114, 2005.

[39] A. P. Roday and M. K. Jensen, Experimental Investigation of the CHF condition during flow boiling of water in microtubes, paper no. HT2007-32837, *2007 ASME-JSME Thermal Engineering Summer Heat Transfer Conference*, Vancouver, British Columbia, Canada, 2007.

[40] A. P. Roday, Study of the critical heat flux condition in microtubes, Ph.D thesis, Rensselaer Poly technic Institute, Troy, NY, 2007.

[41] I. Hasaan, M. Vaillancourt and K. Pehlivan, Two-phase flow regime transitions in microchannels: a comparative experimental study, *Micro scale Thermophysical Engineering*, 9 (2005) 165-182, 2005.

[42] R. Revellin and J. R. Thome, A new type of diabatic flow pattern map for boiling heat transfer in microchannels," *Journal of Micromechanics and Microengineering*, 17 (2007) 788-796.

[43] J. Weisman, The current status of the theoretically based approaches to the prediction of the critical heat

flux in flow boiling," *Nuclear Technology*, 99 (1992) 1-121.

[44] L. S. Tong and Y. S. Tang, Boiling heat transfer and two-phase flow," Taylor and Francis, Washington, DC, 1997.

[45] J. Weisman and B. S. Pei, Prediction of critical heat flux in flow boiling at low qualities, *International Journal of Heat and Mass Transfer*, 26 (11) 1463-1477.

[46] C. H. Lee and I. Mudawar, A phenomenological model for the prediction of critical heat flux under highly subcooled conditions," *Fusion Technology*, 13 (1988) 654-659.

[47] Y. Katto, Prediction of critical heat flux of sub cooled flow boiling in round tubes, *International Journal of Heat and Mass Transfer*, 33 (1990) 1921-1928.

[48] G. P. Celata, M. Cumo. A. Mariani, M. Simoncini and G. Zummo, Rationalization of existing mechanistic models for the prediction of water subcooled flow boiling critical heat flux, *International Journal of Heat and Mass Transfer*, 37 (1) (1994) 347-360.

[49] J. E. Galloway and I. Mudawar, CHF mechanism in flow boiling from a short heated wall—II. Theoretical CHF model, *International Journal of Heat and Mass Transfer*, 36 (1993) 2527-2540.

[50] G. F. Hewitt and A. H. Govan, Phenomena and prediction in annular two-phase flow, *ASME Advances in Gas-Liquid Flows*, FED 99 (1990) 41-56.

[51] S. Sugawara, Droplet deposition and entrainment modeling based on the three-fluid model, *Nuclear Engineering Design*, 122 (1990) 67-84.

[52] J. R. Thome, V. Dupont and A. M. Jacobi, Heat transfer model for evaporation in microchannels. Part I: presentation of the model," *International Journal of Heat and Mass Transfer*, 47 (2004) 3375-3385.

[53] S. G. Kandlikar, A theoretical model to predict pool boiling CHF incorporating effects of contact angle orientation," *ASME Journal of Heat Transfer*, 123 (2001) 1071-1079.

[54] R. Revelli and J. R. Thome, A theoretical model for the prediction of the critical heat flux in heated microchannels, *International Journal of Heat and Mass Transfer*, in press.

[55] D. D. Hall and I. Mudawar. Critical heat flux (CHF) for water flow in tubes–II. Subcooled CHF correlations, *International Journal of Heat and Mass Transfer*, 43 (2000) 2605-2640.

[56] I. Mudawar and M. B. Bowers, Ultra-high critical heat flux (CHF) for subcooled water flow boiling—I: CHF data and parametric effects for small diameter tubes, *International Journal of Heat and Mass Transfer*, 42 (1999) 1405-1428.

[57] A. E. Bergles, R. F. Lopina and M. P. Fiori, Critical-Heat-Flux and Flow-Pattern Observations for Low-Pressure Water Flowing in Tubes, *Journal of Heat Transfer*, 69-74, 1967.

[58] W. Zhang, T. Hibiki, K. Mishima and Y. Mi, Correlation of critical heat flux for flow boiling of water in mini-channels," *International Journal of Heat and Mass Transfer*, Winfrith, U.K., 1972, 49 (2006) 1058-1072.

Anand P. Roday completed his PhD in Mechanical Engineering from Rensselaer Polytechnic Institute, Troy, NY USA. Earlier he obtained his Master's degree from the University of Cincinnati, OH, USA where he worked on the analysis of thermal energy storage systems. His research during PhD was focused on flow boiling in microchannels. He has a six year industrial work experience in India prior to his graduate studies. His research interests lie in the areas of solid-liquid phase change and boiling heat transfer. He is a member of ASME.

Michael K. Jensen is a professor in the Department of Mechanical, Aerospace, and Nuclear Engineering at Rensselaer Polytechnic Institute, Troy, NY USA. His research interests have been directed toward convective single- and two-phase heat transfer and the associated fluid flows with an emphasis on these processes in heat exchangers and using enhanced heat transfer techniques. Recent research has focused on microdomain heat transfer and thermal management of electronic systems, solar energy, and fuel cells; over 130 archival technical papers have resulted from this research. He has received several teaching awards, served on editorial boards of four international journals, chaired the ASME Heat Transfer Division, and has chaired/co-chaired six international conferences.